Electronic Supplementary Information (ESI)

Modulation of the driving forces for adsorption of MIL-101 analogues by decoration with sulfonic acid functional groups: Superior selective adsorption of hazardous anionic dyes

Ji-Min Yang*, Wei Zhang, Run-Zhi Zhang and Meng-Xuan Tong

School of Chemistry & Chemical Engineering, Linyi University, Linyi 276005, China

* Corresponding author: Tel.: +86 539 7258620; fax: +86 539 7258620; e-mail: yangjimin@lyu.edu.cn

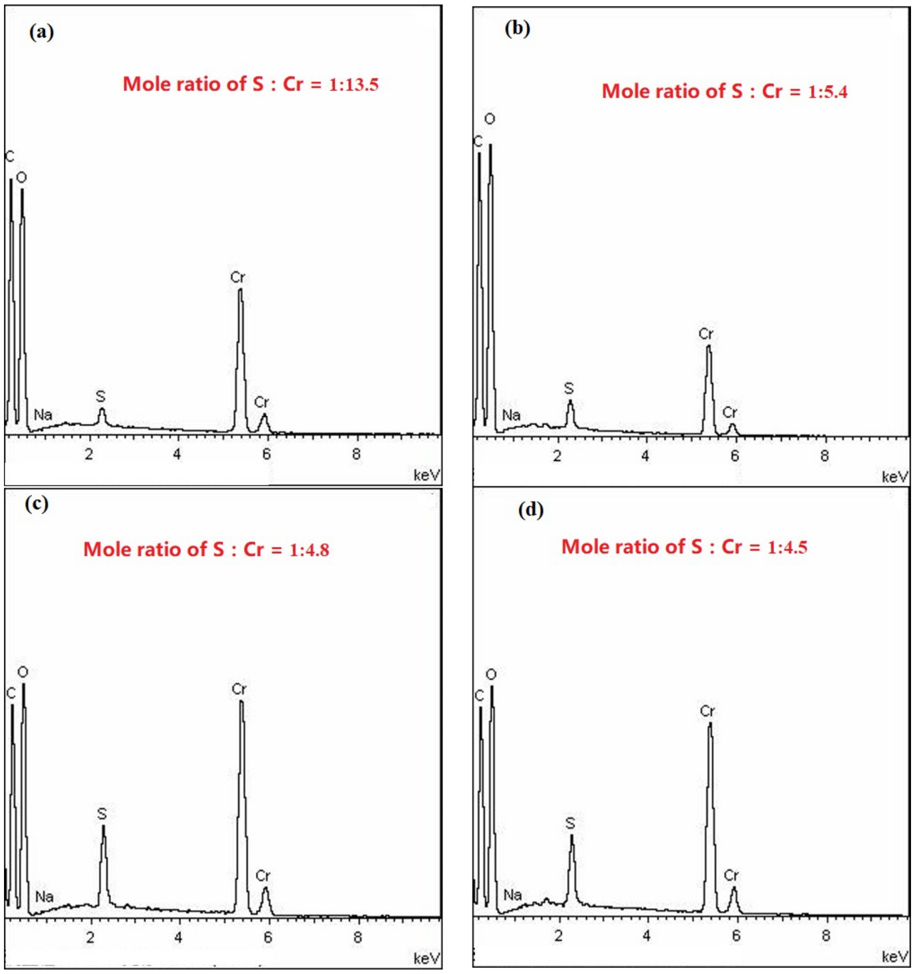

Fig. S1 EDS spectra of MIL-101-SO_3H products synthesized with different mole ratio of H_2BDC-SO_3Na : H_2BDC: (a) 1 : 9, (b) 2 : 8, (c) 3 : 7 and (d) 4 : 6..

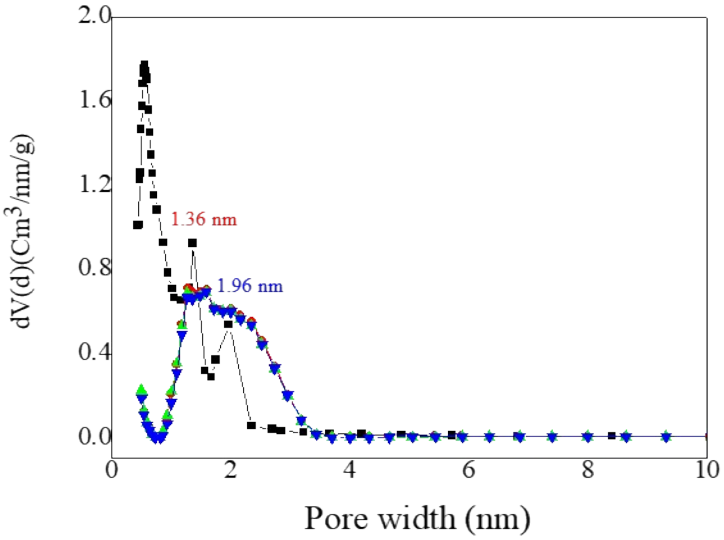

Fig. S2 The pore size distributions of MIL-101-SO_3H.

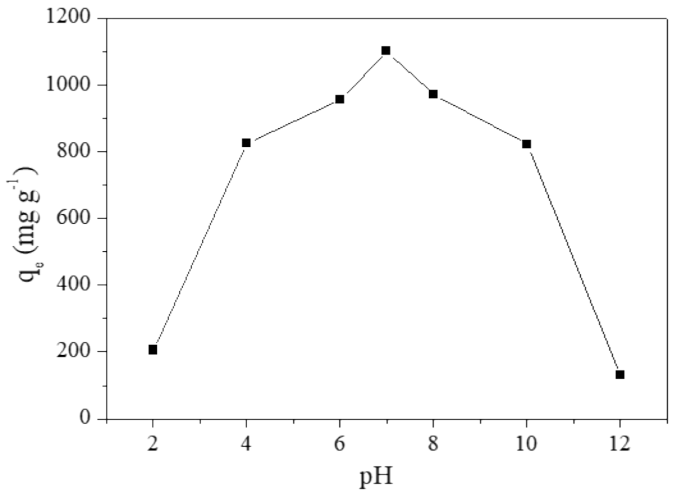

Fig. S3 Effect of pH on CR adsorption on theMIL-101-SO_3H-1 microcrystals.

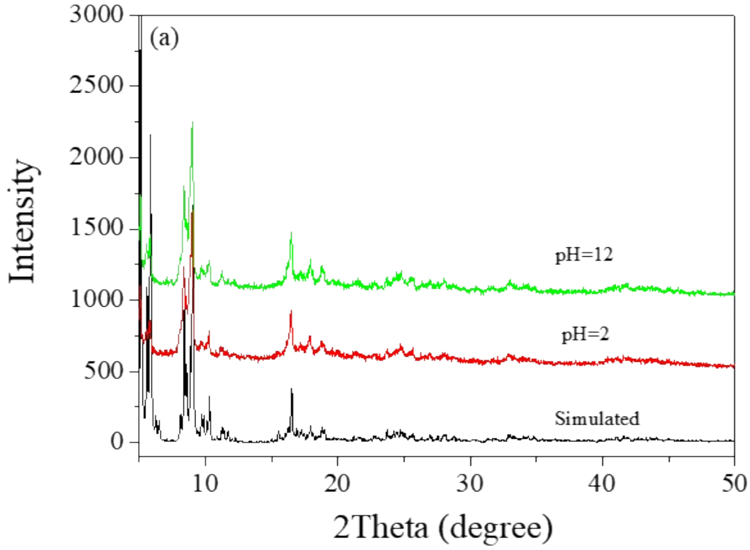

Fig. S4 Simulated and experimental powder XRD patterns at different pH.

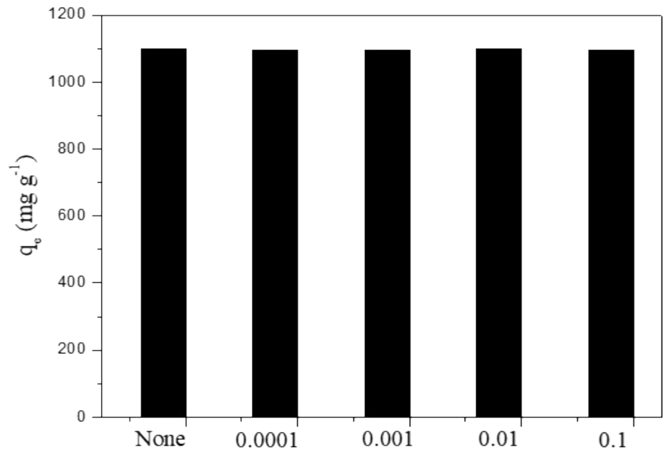

Fig. S5 Adsorption capacity of CR with different concentrations of Na^+ ion.

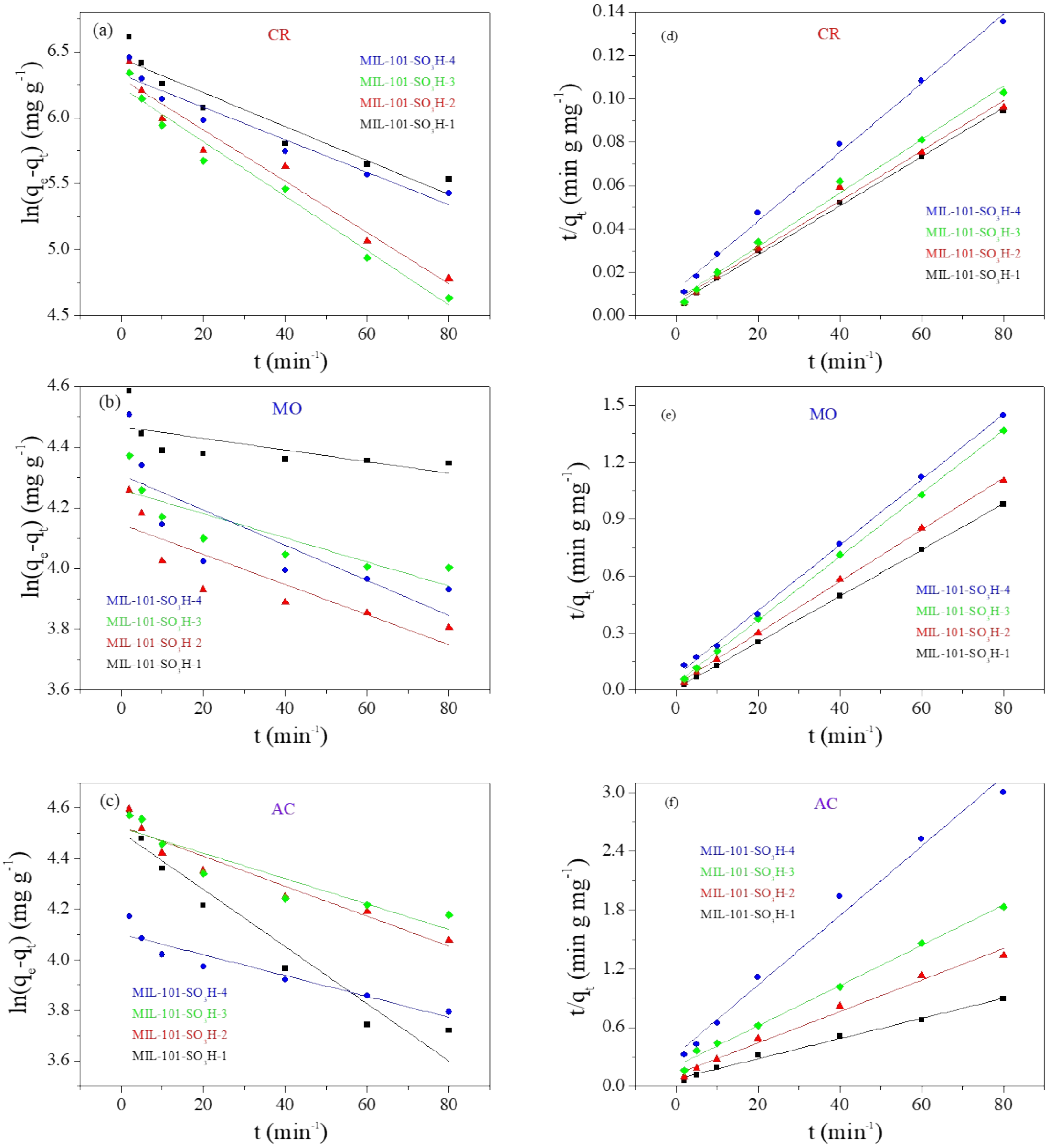

Fig. S6 (a–c) Pseudo-first-order and (d–f) pseudo-second-order fits of the experimental adsorption kinetic data.

Table S1 Characteristic parameters of the adsorption of dyes on the MIL-101-SO_3H-1.

		parameters	CR	MO	AC
Adsorption kinetics	Pseudo-first-order	$q_{e,Exp}$ (mg g^{-1})	1099.2	158.9	130.9
		$q_{e,Cal}$ (mg g^{-1})	630.6	82.2	90.4
		k_1 (min^{-1})	0.0129	0.0019	0.0113
		R^2	0.8958	0.3541	0.9237
	Pseudo-second-order	$q_{e,Exp}$ (mg g^{-1})	1099.2	158.9	130.9
		$q_{e,Cal}$ (mg g^{-1})	884.9	87.1	97.1
		k_2 (g mg^{-1} min^{-1})	2.4×10^{-4}	1.8×10^{-2}	1.4×10^{-3}
		R^2	0.9977	0.9999	0.9926
Adsorption isotherm	Tempkin	A (L g^{-1})	9.9	1.5	40.9
		B	346.4	110.3	22.1
		R^2	0.9680	0.8775	0.9513
	Freundlich	n	3.1	3.4	7.8
		k_F (mg g^{-1} (L $mg^{-1})^{1/n}$)	553.0	135.9	100.0
		R^2	0.9219	0.7941	0.9621
	Langmuir	$q_{m,Exp}$ (mg g^{-1})	2592.7	688.9	213.2
		$q_{m,Cal}$ (mg g^{-1})	2620.8	699.3	219.3
		b (L mg^{-1})	0.2327	0.0607	0.0802
		R^2	0.9994	0.9977	0.9990
Thermodynamic constant		ΔG (kJ mol^{-1})	-3.6	-6.9	-6.3

Table S2 Characteristic parameters of the adsorption of dyes on the MIL-101-SO_3H-2.

		parameters	CR	MO	AC
Adsorption kinetics	Pseudo-first-order	$q_{e,Exp}$ (mg g^{-1})	952.9	117.4	118.9
		$q_{e,Cal}$ (mg g^{-1})	542.3	63.2	62.3
		k_1 (min^{-1})	0.0194	0.0049	0.0059
		R^2	0.9528	0.7016	0.9142
	Pseudo-second-order	$q_{e,Exp}$ (mg g^{-1})	952.9	117.4	118.9
		$q_{e,Cal}$ (mg g^{-1})	862.1	73.4	92.5
		k_2 (g mg^{-1} min^{-1})	2.0×10^{-4}	6.9×10^{-3}	2.1×10^{-3}
		R^2	0.9891	0.9993	0.9865
Adsorption isotherm	Tempkin	A (L g^{-1})	7.2	0.4	1035.1
		B	260.7	100.2	12.5
		R^2	0.9660	0.9642	0.8791
	Freundlich	n	3.4	1.5	11.3
		k_F (mg g^{-1} (L $mg^{-1})^{1/n}$)	427.4	75.3	94.8
		R^2	0.8075	0.9411	0.8942
	Langmuir	$q_{m,Exp}$ (mg g^{-1})	1962.0	550.4	165.1
		$q_{m,Cal}$ (mg g^{-1})	1993.9	578.0	169.2
		b (L mg^{-1})	0.1276	0.0199	0.0692
		R^2	0.9971	0.9737	0.9982
Thermodynamic constant		ΔG (kJ mol^{-1})	-5.1	-9.7	-6.6

Table S3 Characteristic parameters of the adsorption of dyes on the MIL-101-SO_3H-3.

		parameters	CR	MO	AC
Adsorption kinetics	Pseudo-first-order	$q_{e,Exp}$ (mg g^{-1})	880.1	113.3	105.9
		$q_{e,Cal}$ (mg g^{-1})	507.6	60.1	48.7
		k_1 (min^{-1})	0.0206	0.0039	0.0050
		R^2	0.9702	0.6819	0.8266
	Pseudo-second-order	$q_{e,Exp}$ (mg g^{-1})	880.1	113.3	105.9
		$q_{e,Cal}$ (mg g^{-1})	813.1	70.8	92.0
		k_2 (g mg^{-1} min^{-1})	2.1×10^{-4}	7.6×10^{-3}	2.0×10^{-3}
		R^2	0.9919	0.9997	0.9936
Adsorption isotherm	Tempkin	A (L g^{-1})	4.1	0.6	21801.1
		B	243.8	70.2	8.4
		R^2	0.9645	0.9731	0.9007
	Freundlich	n	3.2	3.4	14.4
		k_F (mg g^{-1} (L $mg^{-1})^{1/n}$)	335.8	68.2	88.3
		R^2	0.7868	0.9813	0.9182
	Langmuir	$q_{m,Exp}$ (mg g^{-1})	1699.1	423.3	138.9
		$q_{m,Cal}$ (mg g^{-1})	1732.4	440.5	140.3
		b (L mg^{-1})	0.1087	0.0230	0.0772
		R^2	0.9966	0.9889	0.9979
Thermodynamic constant		ΔG (kJ mol^{-1})	-5.5	-9.3	-6.3

Table S4 Characteristic parameters of the adsorption of dyes on the MIL-101-SO_3H-4.

		parameters	CR	MO	AC
Adsorption kinetics	Pseudo-first-order	$q_{e,Exp}$ (mg g^{-1})	817.1	106.2	71.1
		$q_{e,Cal}$ (mg g^{-1})	588.3	58.7	28.2
		k_1 (min^{-1})	0.0123	0.0058	0.0041
		R^2	0.9271	0.5678	0.8750
	Pseudo-second-order	$q_{e,Exp}$ (mg g^{-1})	817.1	106.2	71.1
		$q_{e,Cal}$ (mg g^{-1})	628.9	74.3	60.5
		k_2 (g mg^{-1} min^{-1})	2.1×10^{-4}	3.9×10^{-3}	3.8×10^{-3}
		R^2	0.9947	0.9990	0.9845
Adsorption isotherm	Tempkin	A (L g^{-1})	2.18	0.48	2.1×10^{4}
		B	197.6	63.2	12.1
		R^2	0.9564	0.9767	0.9239
	Freundlich	n	2.9	3.3	7.6
		k_F (mg g^{-1} (L mg^{-1})$^{1/n}$)	207.6	57.5	49.7
		R^2	0.94487	0.9801	0.9571
	Langmuir	$q_{m,Exp}$ (mg g^{-1})	1281.8	357.9	116.5
		$q_{m,Cal}$ (mg g^{-1})	1332.1	378.8	119.0
		b (L mg^{-1})	0.0656	0.0210	0.0378
		R^2	0.9974	0.9839	0.9916
Thermodynamic constant		ΔG (kJ mol^{-1})	-6.8	-9.6	-8.1

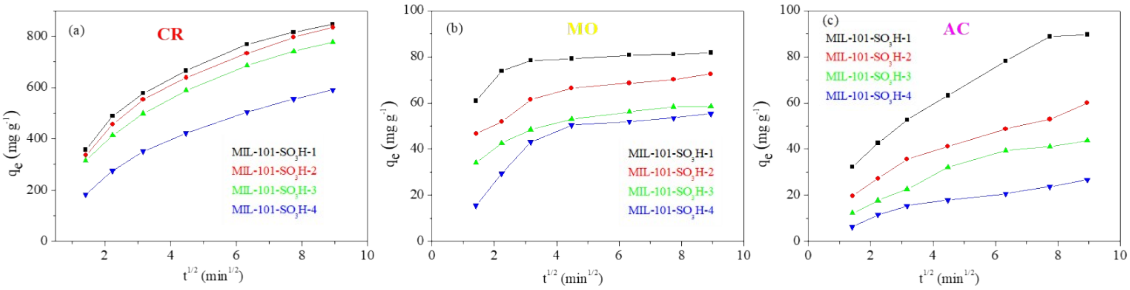

Fig. S7 Weber–Morris intra-particle diffusion plots for the adsorption of (a) CR, (b) MO and (c) AC on the MIL-101-SO_3H micro/nanoparticles.

Table S5 Summary of CR maximum adsorption capacities (*q*) on various adsorbents.

Type of adsorbent	*q* (mg g^{-1})	Reference
MIL-101-SO_3H-1	2592.7	This work
MIL-101-SO_3H-2	1962.0	This work
UiO-67	1236.9	39
MIL-68(In)	1204	40
Ni-Cu-BTC	999.2	41
Mesoporous alumina fibers	781.3	42
$[Co(L_2)(Htp)(tp)_{0.5}]_n$	629.6	43
Hierarchical hollow NiO	440	44
a-FeOOH	275	45
Activated carbon	200	46

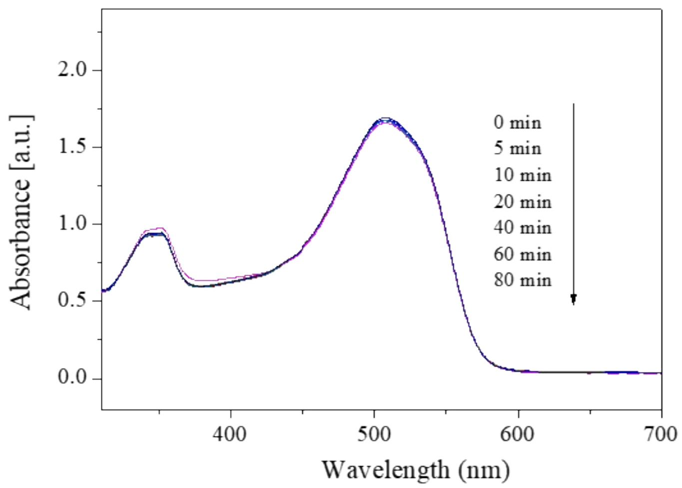

Fig. S8 The adsorption rate with MIL-101(Cr) (5 mg) for SD (20 mg/L, 50 mL).

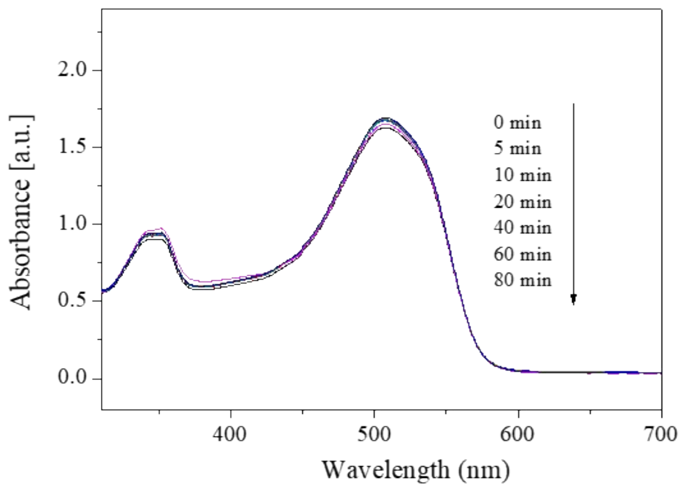

Fig. S9 The adsorption rate with MIL-101-SO_3H-1 (5 mg) for SD (20 mg/L, 50 mL).

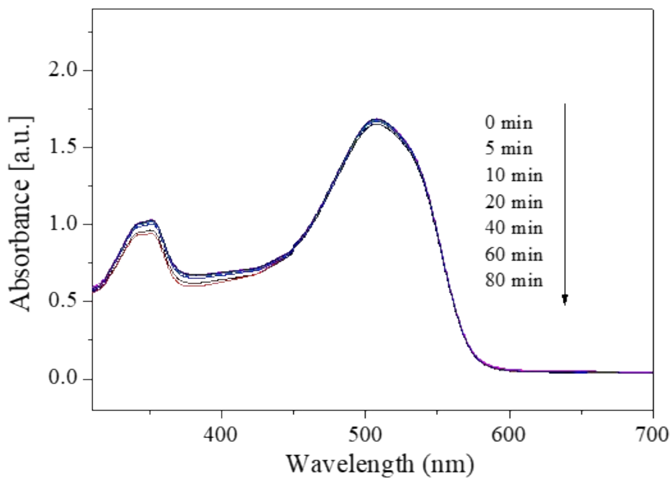

Fig. S10 The adsorption rate with MIL-101-SO_3H-4 (5 mg) for SD (20 mg/L, 50 mL).

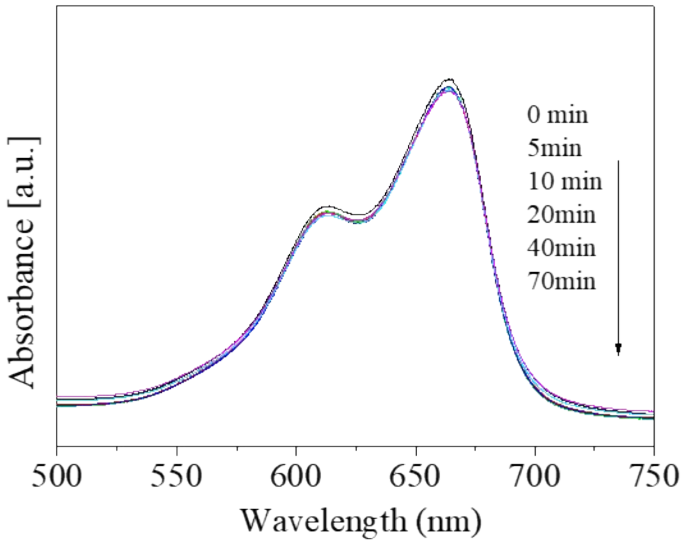

Fig. S11 The adsorption rate with MIL-101(Cr) (5 mg) for MB (20 mg/L, 50 mL).

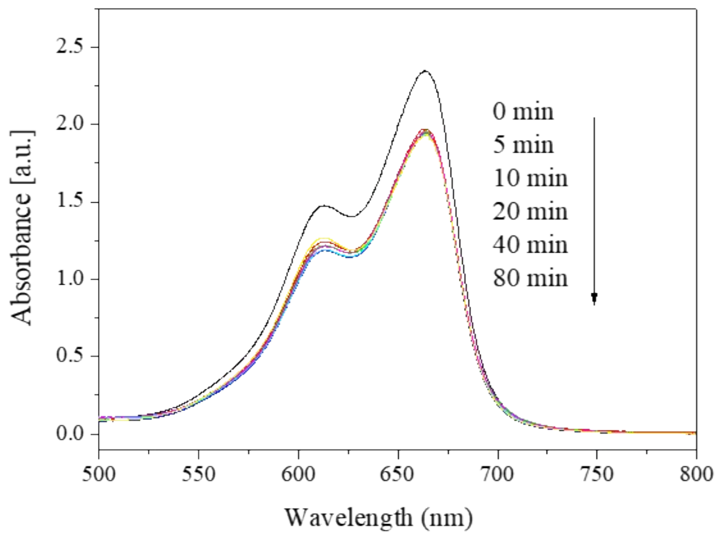

Fig. S12 The adsorption rate with MIL-101-SO_3H-1 (5 mg) for MB (20 mg/L, 50 mL).

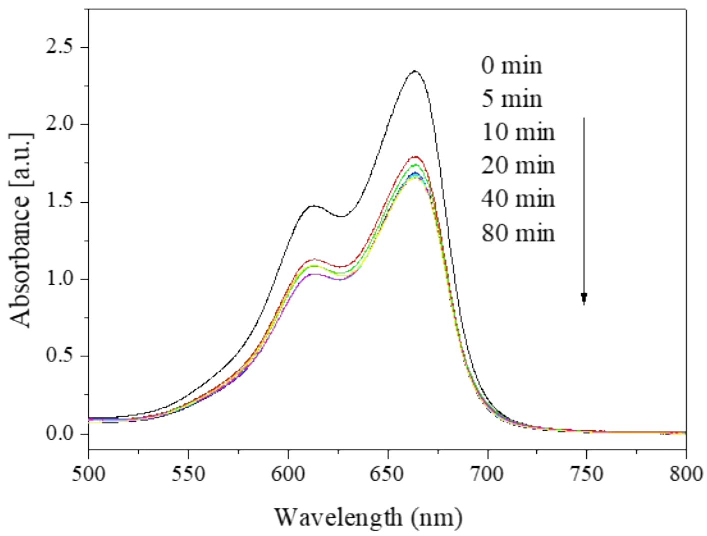

Fig. S13 The adsorption rate with MIL-101-SO_3H-4 (5 mg) for MB (20 mg/L, 50 mL).

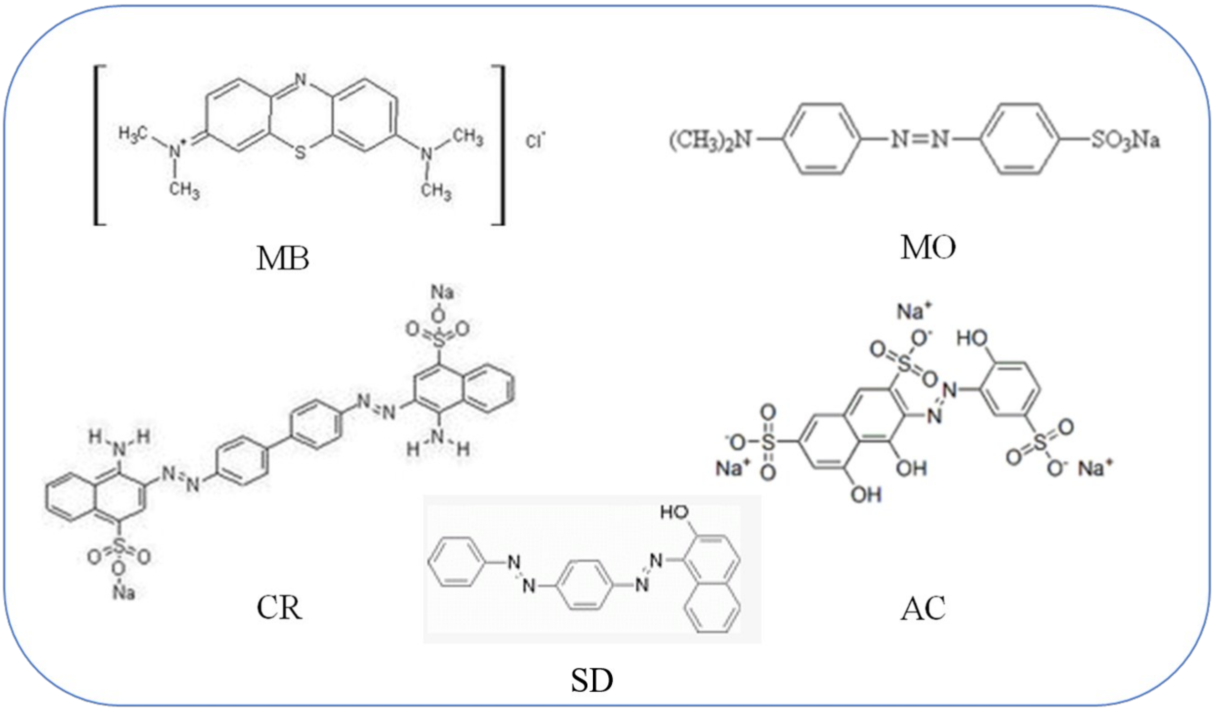

Fig. S14 Molecular structures of the investigated dyes.

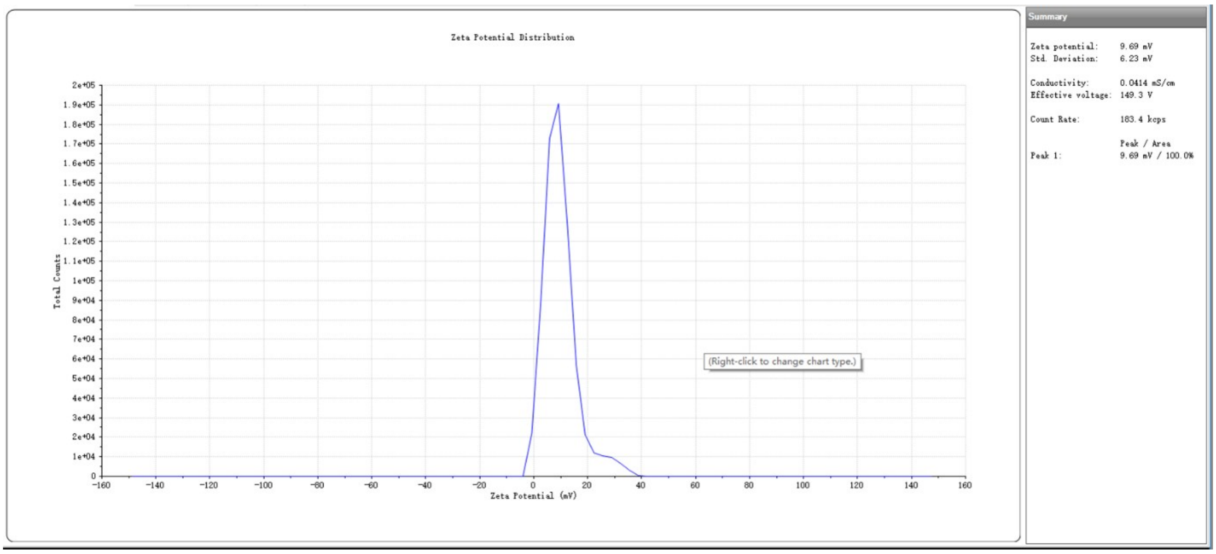

Fig. S15 Zeta potential of MIL-101-SO_3H-1 microparticles directly dispersed in water.

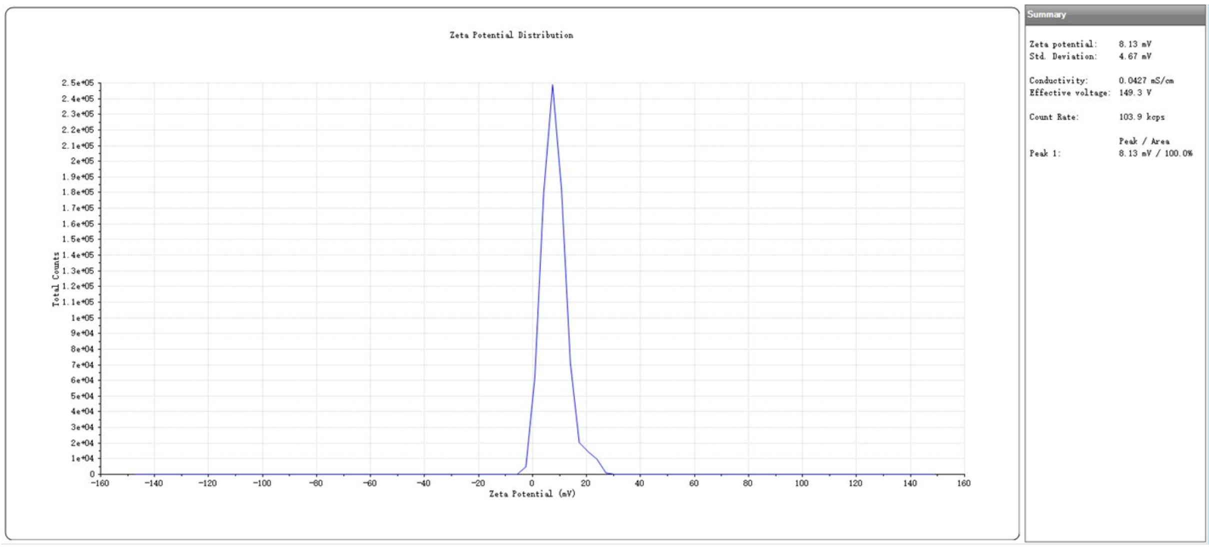

Fig. S16 Zeta potential of MIL-101-SO_3H-2 microparticles directly dispersed in water.

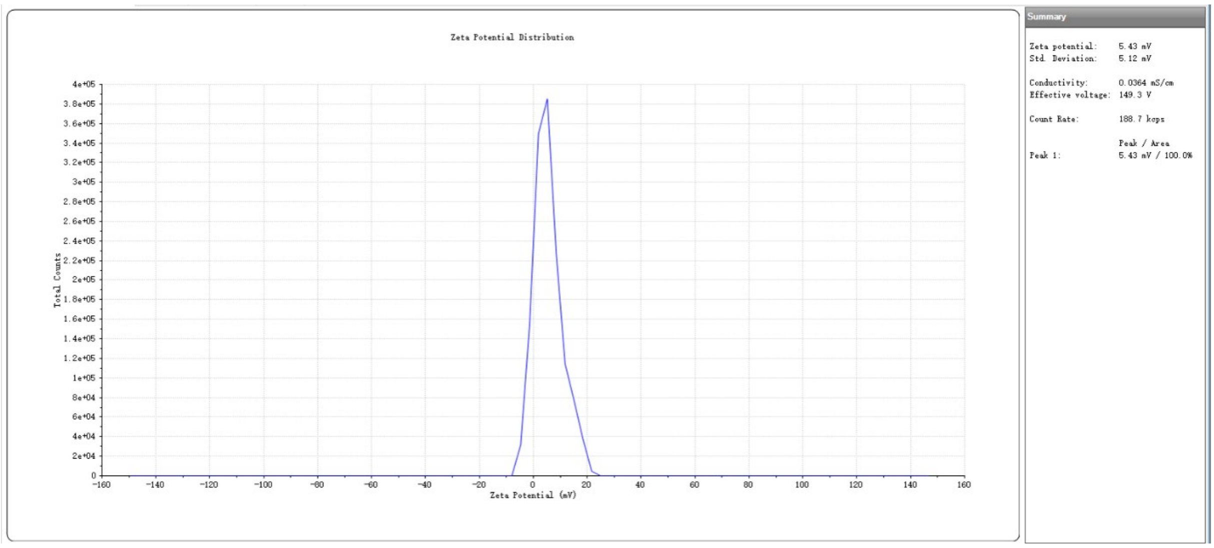

Fig. S17 Zeta potential of MIL-101-SO_3H-3 microparticles directly dispersed in water.

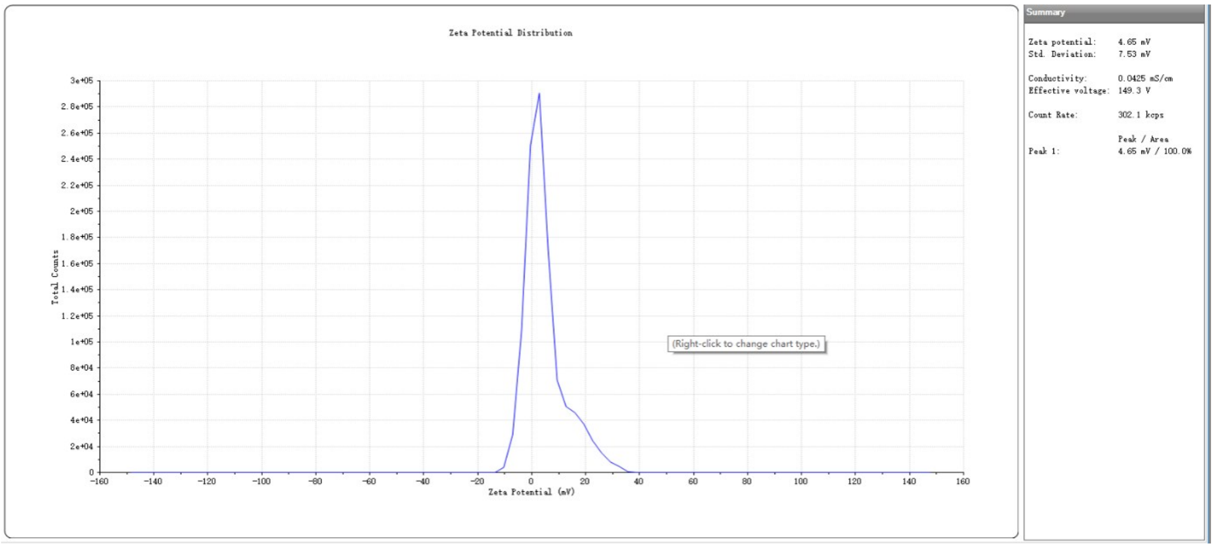

Fig. S18 Zeta potential of MIL-101-SO_3H-4 nanoparticles directly dispersed in water.

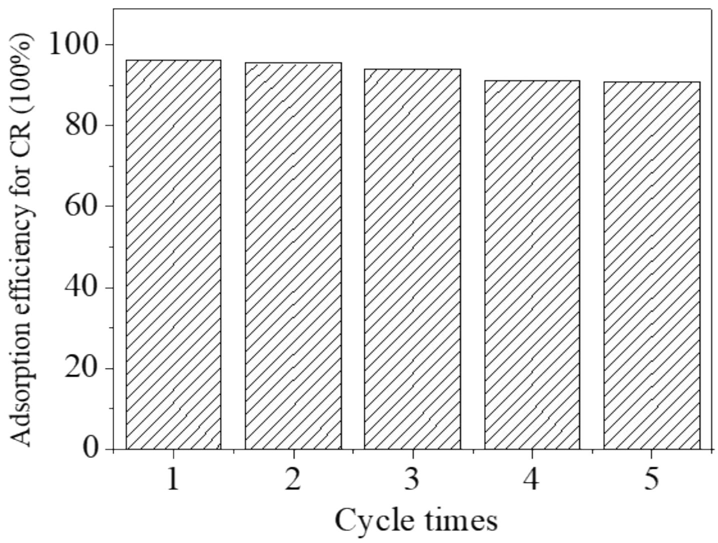

Fig. S19 Recycle of the removal efficiency of MIL-101-SO_3H-1 for CR.

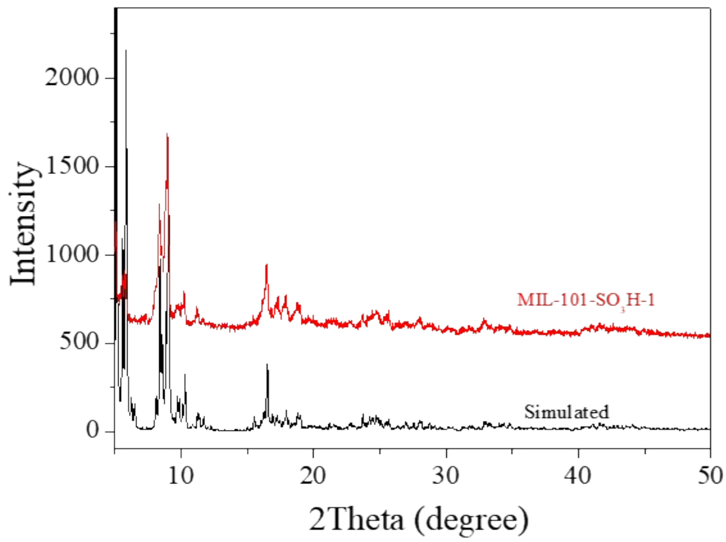

Fig. S20 PXRD patterns of the MIL-101-SO_3H-1 microparticles after regeneration.